12-1994

An Experimental Apparatus for Studying Double Differential Scattering by Low-Energy Multiply Charged Ions from Atomic Targets

Meenatchi S. Gopinathan

AN EXPERIMENTAL APPARATUS FOR STUDYING DOUBLE DIFFERENTIAL SCATTERING BY LOW-ENERGY MULTIPLY CHARGED IONS FROM ATOMIC TARGETS

by

Meenatchi S. Gopinathan

A Thesis
Submitted to the
Faculty of The Graduate College
in partial fulfillment of the
requirements for the
Degree of Masters of Arts
Department of Physics

Western Michigan University
Kalamazoo, Michigan
December 1994

ACKNOWLEDGMENTS

First of all I would like to thank my parents for their love, affection and support for my higher studies in USA, though we were separated by large geographic distance.

I also wish to thank my advisor, Dr. E. Y. Kamber, for his patient guidance and instruction without whose help this thesis could never been completed. I also wish to thank other members of my committee Dr. J. A. Tanis, and Dr. S. M. Ferguson for their valuable comments and suggestions about my thesis. My Thanks also goes to my friends, Kadir Akgungor and John Edens, for their friendship and support.

Meenatchi S. Gopinathan

AN EXPERIMENTAL APPARATUS FOR STUDYING DOUBLE DIFFERENTIAL SCATTERING BY LOW-ENERGY MULTIPLY CHARGED IONS FROM ATOMIC TARGETS

Meenatchi S. Gopinathan, M.A.

Western Michigan University, 1994

A new differential energy-gain spectrometer with a movable parallel-plate electrostatic energy analyzer has been constructed and tested for the study of double differential (in energy and angle) cross sections for state-selective electron capture processes in collisions of low-energy multiply charged ions with atomic gases. The ion beam is produced by extracting recoil ions from a primary interaction region where these ions are generated in collisions between a neutral target gas and a fast fluorine beam from the WMU tandem Van de Graaff accelerator. An einzel lens is used to focus the ion beam extracted from the recoil-ion source into a 180^0 double-focussing magnet. After mass and charge selection, the desired ion beam is steered through a gas collision cell containing the target gas. Scattered ions are energy analyzed by a 45^0 parallel-plate electrostatic energy analyzer and detected with a channel electron multiplier. Here we describe the experimental apparatus for studying double differential cross-sections and discuss a few specific collision systems.

TABLE OF CONTENTS

Table of Contents-Continued

LIST OF TABLES

LIST OF FIGURES

CHAPTER I

INTRODUCTION

The intention of this thesis is to describe the design, the construction, and the testing of a doubly differential energy-gain spectrometer using a movable parallel-plate electrostatic energy analyzer, and, additionally, to conduct a preliminary investigation of single electron capture by measuring the energy gained by low-energy projectile ions in collisions with atomic targets at different scattering angles.

Single-electron capture processes in which a bound electron is transferred from the target atom to the projectile ion can be represented as

$$A^{q+}+B\text{------}\rightarrow A^{q-1}+B^{+}+\Delta E \qquad (1.1)$$

where q is initial charge of the projectile,

q-1 is final charge of the projectile,

Δ E is the energy defect of the reaction channel.

This process is also referred to as charge exchange or charge transfer. The study of ion-atom or ion-molecule collisions at low impact energies is generally referred to as collision spectroscopy. However, when the collision is

studied by measuring the post-collision kinetic energy of the projectile ion, the technique is more specifically called translational energy spectroscopy.

Collision studies have been broadly classified by the velocity of the incident projectile ion. If the incident ion velocity is greater than the orbital velocity of electrons about the target nucleus then it is called a high-velocity collision and if the ion velocity is less than the orbital velocity, then it is a low-velocity collision. Our main area of interest here is low-velocity collisions.

Single-electron capture in collisions between multiply-charged ions and atoms is currently an active field of research. Plasma models used in astrophysics, both for hot plasmas (like the sun) and cold plasmas(such as planetary nebulae) depend critically on the cross section for electron capture and on the decay rates for excited ions (Dalgarno and Butler 1978, Dalgarno 1985). Also these kinds of collisions are relevant to the construction of extreme ultraviolet(EUV) and soft x-ray lasers, where recombining collisions are expected to produce level inversions which can be used for lascent schemes (Peacock and Summer 1987). Electron capture also plays an important role in accelerator design, the physics of the upper atmosphere, development of particle detectors, etc.

Concerning laboratory plasmas, there is still a considerable demand for accurate data on collisions involving multiply-charged ions in thermonuclear fusion research (Drawin 1981). These data are required for plasma diagnostics (Suckewar 1981, Isler et al., 1985, Duval et al., 1985, carolan et al., 1987, Donne and De Heer 1987) and for a determination of the feasibility of fast neutral beam heating in large tokamak machines.

Several experimental measurements on electron capture from rare gas atoms by multiply-charged ions using translational energy spectroscopy have been reported. Nielsen et al. (1985) measured absolute state-selective single-electron capture cross sections for 1 keV Ar^{q+} ($6 \leq q \leq 10$) ions on Ne, Ar, and Xe by means of energy-gain spectroscopy. Puerta et al. (1985) studied single-electron capture by 200q eV Ar^{q+} ions (q=3 and 4) from rare gas targets. Afrosimov et al. (1986) measured the kinetic energy distributions, using coincidence techniques, of both particles after collision of Ar^{q+} ions ($3 \leq q \leq 7$) with He. McCullough et al., (1987) have used translational energy-gain spectroscopy to study, at 1q keV and 2q keV, distributions of excited-product ion channels for single-electron capture by Ar^{q+} ($4 \leq q \leq 6$) ions in H, H_2 and He. Kamber et al. (1987a) have measured single and double electron capture into selected states by means of translational energy-gain

spectroscopy for collisions of 12 keV Ar^{4+} and 15 keV Ar^{5+} with He, Ne, Ar. Recently Yaltkaya et al., (1993) have used translational energy-gain spectroscopy to find the double differential cross sections for state-selective electron capture by 125-500 eV Ar^{4+} and Ar^{5+} from He and Ar target atoms.

The contents of this thesis are as follows. Chapter II describes the theoretical considerations. Chapter III describes the experimental apparatus, energy resolution of the parallel-plate electrostatic energy analyzer, and data acquisition. Chapter IV presents the data analysis. A discussion of the results and comparison with other studies is presented in Chapter V. Finally, Chapter VI summarizes the work, and possible extensions of the experiments are considered.

CHAPTER II

THEORETICAL CONSIDERATIONS

Kinematics

In a classical two-body collision, the translational energy of an ion undergoing an inelastic collision process, $E_{inelastic}$, differs from the energy of the projectile ion E_o by

$$E_{inelastic}-E_0=\Delta E-\Delta K=Q \qquad (2.1)$$

Where ΔK is the translational energy given to the target and ΔE is the energy defect of the reaction. The parameter Q is the total change in internal energy that takes places during the inelastic collision. This parameter is called the energy gain or loss of the collision and can be negative (endothermic reaction) or positive (exothermic reaction) depending on the binding energy of the captured electron. The Q value can also be zero. A typical charge exchange reaction at low collision energy in the laboratory system is shown in Figure 1, in which the projectile ion is scattered through an angle θ_p while the recoil target ion is scattered through an angle θ_r measured from 90^o. At low collision energies the resulting positive charge of the

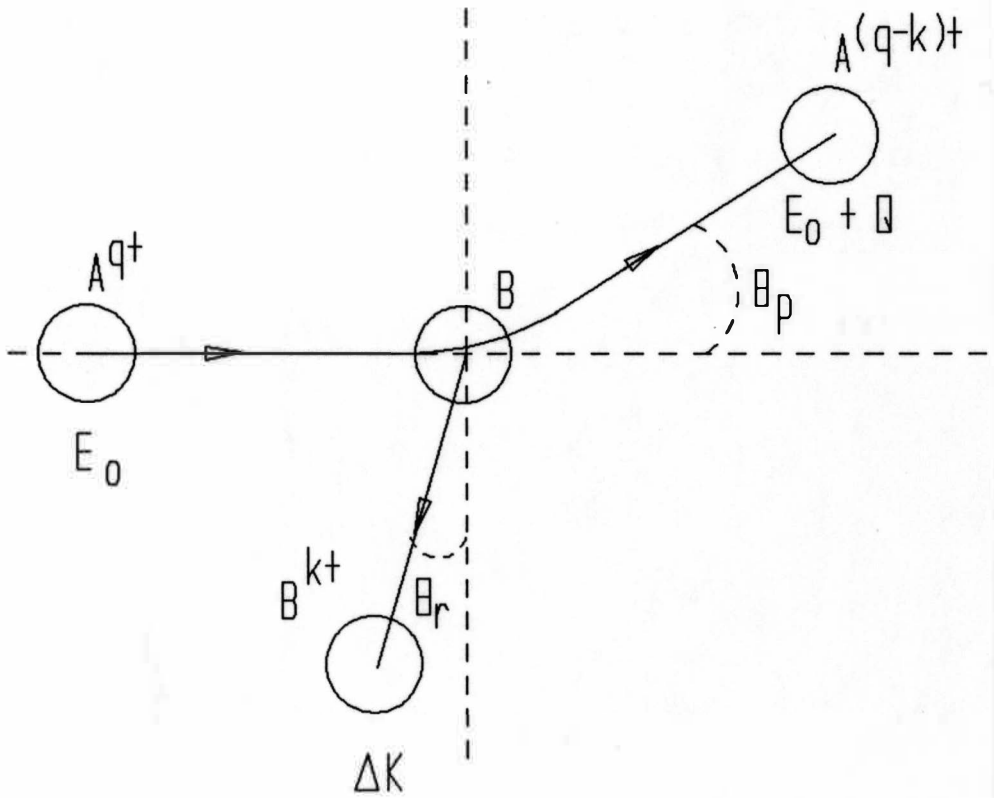

Figure 1. Typical Charge Exchange Reaction in the Laboratory Frame.

target normally gives rise to a small backward component of momentum for the target ion (Cooks 1978, Giese et al., 1986).

The parameter ΔE is calculated according to the formula

$$\Delta E = I_p(A^{(q-k)+}) - I_p(B^{k+}) - E_j \qquad (2.2)$$

where $I_p(A^{(q-k)+})$ is the ionization potential of the projec-

tile product ions, $I_p(B^{k+})$ is the ionization potential of the target ion after the collision, k is the number of electrons transferred, and E_j is the excitation energy of the electron after it is captured.

The translational energy ΔK given to the target is calculated according to the formula

$$\Delta K = \frac{m_p}{m_p+M}(1 - \cos\theta_p)\left[\frac{2ME_o}{m_p+M} - \Delta E\right] + \frac{m_p(\Delta E)^2}{4ME_o}\cos\theta_p \quad (2.3)$$

where m_p is the projectile mass, M is the target mass, and E_o and θ_p are, respectively, the initial laboratory translational energy of the projectile and the final laboratory scattering angle of the projectile (Cooks, 1978).

If the scattering angle θ_p of the projectile is close to zero, ΔK can be expressed by

$$\Delta K = m_p(\Delta E)^2/4ME_0. \quad (2.4)$$

In the present measurements the projectile ions lose relatively little translational energy in an electron capture process, i.e, $\Delta K \leq 1$ eV. Thus the energy defect ΔE in an inelastic process is conveniently expressed in terms of the internal energy change Q.

Olson and Kimura (1982) have pointed out the importance of angular scattering in collisions between slow

multiply-charged ions and atoms. To estimate this effect we have adopted the simple procedure suggested by Nielsen et al., (1985). In this model it is assumed there is no interaction in the incoming (entrance) channel and Coulomb scattering only in the outgoing (exit) channel, and a well defined impact parameter b corresponding to the energy defect ΔE,

$$b=\frac{(q-k)\,ke^2}{\Delta E} \qquad (2.5)$$

where q-k and k are the charge states of the two products after the interaction. In the center-of-mass system, the scattering angle in such a Coulomb collision is given as

$$\tan\Phi=\frac{1}{2}\left(1+\frac{m_p}{M}\right)\frac{\Delta E}{E_0} \qquad (2.6)$$

and the scattering angle θ in the laboratory system ($Q/E_0 << 1$) is, given by

$$\tan\Theta=\frac{\sin\Phi}{\cos\Phi+\frac{m_p}{M}} \qquad (2.7)$$

In this work, we are interested only in cases where both angles are small and we obtain the following simple expression for the laboratory scattering angle associated with electron capture,

$$\Theta = \frac{Q}{2E_0} \tag{2.8}$$

Landau-Zener Model

A schematic of the potential energy curves associated with a single-electron capture process is shown in Figure 2. The incoming channel $A^{q+} + B$ and the outgoing channel $A^{q-1} + B^{+}$ intersect at some crossing radius R_x given by the solution of the equation (in atomic units)

$$Q = V_o(R_x) - V_i(R_x) \tag{2.9}$$

If polarization of the target is neglected, the incoming potential V_i can be set equal to zero. The outgoing potential V_o is given by the Coulomb formula

$$V_o = \frac{k(q-k)}{} \tag{2.10}$$

and the crossing radius is then,

$$R_x = \frac{k(q-k)}{Q}. \tag{2.11}$$

Transitions from the incoming channel to the outgoing channel are enhanced by strong interactions occurring at the curve crossings. According to the Landau-Zener model

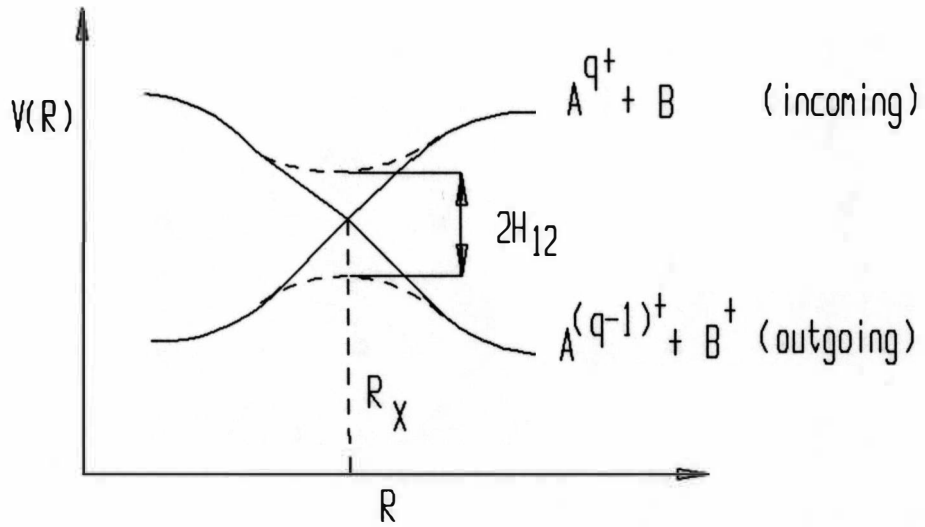

Figure 2. Schematic plot of the Potential Energy V(R) Curves for the Incoming and Outgoing Channels Near a Curve Crossing Versus Internuclear Separation R; ---, Adiabatic Basis; ——, Diabatic Basis.

The Coupling Matrix Element H_{12} is One-Half the Adiabatic Splitting at the Crossing Radius.

(Kamber et al., 1991), the single-crossing transition probability at each crossing R_x is

$$P_n = \exp(-2\pi H_{12}^2 / v_r \Delta F) \qquad (2.12)$$

where H_{12} is the coupling matrix element and is approximately equal to one-half the adiabatic splitting (when the internuclear separation varies infinitely slowly there are no transitions between the two states) at R_x and ΔF is the difference in slopes of the diabatic potential curves at

the curve crossing (Kimura et al., 1984). In the straight-line trajectory approximation (in which it is assumed that the projectile ion is not deflected by the target atomic nucleus) the radial velocity v_r at the internuclear separation R_x of the curve crossing is given by

$$v_r = v_0 [1 - (\frac{b}{R_x})^2]^{1/2} \qquad (2.13)$$

where b is the impact parameter and v_0 is the relative velocity (Kimura et al., 1984). If one assumes a repulsive Coulomb interaction U_1 in the outgoing (exit) channel and zero interaction U_2 in the incoming (entrance) channel, then it is possible to represent ΔF (Olson and Salop, 1976) by

$$\Delta F = \frac{d}{dR} [U(R)_1 - U(R)_2] \approx \frac{q-1}{R^2} \qquad (2.14)$$

where q is the charge state of the incident ion.

Olson and Salop (1976) have developed a semi-empirical expression for the coupling matrix element applicable to collisions of fully-stripped ions with hydrogen atoms. Empirically, they determined a functional expression for H_{12} given by

$$H_{12}^{OS}=9.13q^{-\frac{1}{2}}\exp(-1.324\alpha R_x q^{-\frac{1}{2}}) \qquad (2.15)$$

where $\alpha = (2\ I_t)^{-1/2}$ and I_t is the ionization potential (in a.u.) of the target. A reduction of H_{12} by 40% has been proposed by Kimura et al. (1984) to fit their experimental results, and Taulbjerg (1986) has suggested a correction term to H_{12} to account for projectiles that are only partially stripped.

When there is only one crossing, as in Figure 2, the total probability for electron capture at a given impact parameter is given by

$$P= 2p(1-p) \qquad (2.16)$$

However, the number of curve crossings can become large for collisions of multiply-charged ions with atoms, i.e., many final states can be populated. The extension of the Landau-Zener model to multichannel systems (i.e., several possible exit channels) has been carried out by Olson and Salop (1975). The probability P_n for capture into the nth final state, assuming that there is no interference between different paths leading to a particular exit channel, is

$$\begin{aligned} P_n = {} & p_1\ p_2 \cdots p_n\ (1-p_n)\ [1+(p_{n+1}p_{n+2}\cdots p_N)^2 + \\ & (p_{n+1}p_{n+2}\cdots p_{N-1})^2\ (1-p_N)^2 + (p_{n+1}p_{n+2} \cdots \\ & p_{N-2})^2 + \cdots + p^2_{n+1}\ (1-p_{n+2})^2 + (1-p_{n+1})^2]. \end{aligned} \qquad (2.17)$$

The predictive abilities of the multi-channel Landau Zener (MCLZ) model could be improved by calculating the coupling matrix H_{12} for individual reaction channels of a specific collision system. Here we used the Taulbjerg expression for H_{12} describing electron capture by partially-stripped ions, which is given by

$$H_{12}=f_{nl}H_{12}^{OS} \tag{2.18}$$

where

$$f_{nl}=\frac{(-1)^{n+l-1}(2l+1)^{1/2}\Gamma(n)}{\Gamma(n+l+1)\Gamma(n-l)^{1/2}} \tag{2.19}$$

and n and l characterize the final orbit of the captured electron.

Reaction Window

The state-selective nature of low-energy electron capture can be interpreted in terms of a 'reaction window' in the crossing radii of the final states. The probability for electron capture at a potential crossing is low for both extremely large (R > 10 a.u.)and extremely small (R < 3 a.u.) crossing radii (refer to equations 2.12, 2.14 & 2.15). The range of intermediate radii where the probability is maximum is called the reaction window. According to Taulbjerg (1986), the location of the reaction window

depends modestly on the relative collision velocity, v_0. The reaction window shifts towards larger internuclear separations R if v_0 is reduced and vice versa.

The concept of a reaction window has been successfully used by several authors (Kamber et al., 1987b) to interpret both total and partial cross section measurements. Typically, the location of the reaction window is calculated as a function of the internuclear separation. This location is then compared to the crossing radii of specific final states. Those crossing radii falling within the reaction window are expected to have the largest cross section. It is also possible to find the location of the reaction window in terms of the Q-values of these final states, using equation (2.11). The latter method is used to draw qualitative conclusions on the relative importance of various final states.

CHAPTER III

EXPERIMENT

Apparatus

The apparatus used to study the energy-gain spectra of multiply-charged ions undergoing single-electron capture consists of a recoil-ion source followed by a mass analyzer, deflecting plates, a target collision cell, a 45° parallel-plate electrostatic energy analyzer, and finally a detector. A full description of the experimental apparatus follows.

In this work a fast fluorine beam from the Western Michigan University (WMU) tandem Van de Graaff accelerator was used to 'pump' a recoil-ion source, i.e., the fluorine beam was focussed onto the target gas resulting in the production of recoil ions which were subsequently used as secondary projectile ions. A general layout of the WMU accelerator laboratory is shown in Figure 3.

Recoil-Ion Production

The beginning point of the fluorine ion beam is the Source of Negative ions by Cesium Sputtering(SNICS). In the SNICS, ionized cesium atoms, heated by a tungsten coil,

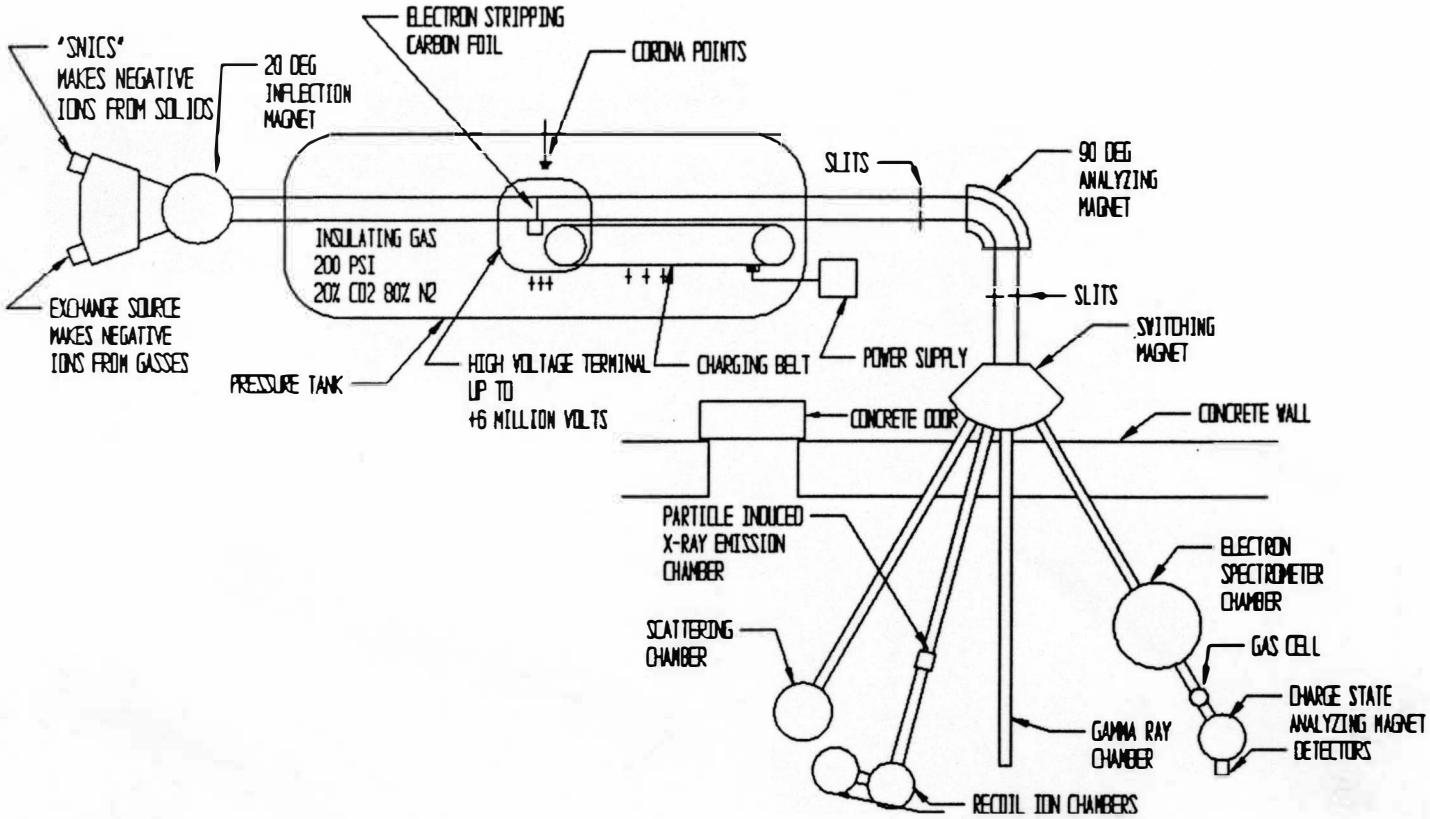

Figure 3. Schematic Diagram of the Western Michigan University Tandem Van de Graaff Accelerator Labortary.

sputter fluorine ions from a calcium fluoride(CaF_2) pellet. We used a fluorine beam because it readily produces negative ions. The sputtered fluorine ions capture electrons due to collisions with cesium atoms in the close vicinity of the cathode, thereby becoming negative ions. These negative ions are repelled by the cathode and accelerated through extraction and focus electrodes located inside the SNICS. Then the negative ion beam passes through the 20^{o} inflection magnet which selects the desired ion (i.e., F^{-}) and directs the fluorine ions into the accelerator beam line. The position of the beam is adjusted using electrostatic steerers and focussed by an Einzel lens before entering the low-energy end of the accelerator. Negative ions are accelerated towards the positively-charged high voltage terminal (up to +6 million volts) in the center of the accelerator and pass through a gas stripper (a foil stripper is also available) where electrons are removed from the ions so that the ions become positively-charged. These positively charged ions are repelled by the terminal voltage and accelerated out of the high-energy end of the accelerator. The accelerator tank contains an insulating gas consisting of a mixture of 20% CO_2 and 80% N_2 at 200 psi. The accelerated beam then passes through the high-energy quadrupole magnet and some defining slits.

The beam emerging from the accelerator consists of several charge states of different beam energies which are analyzed by a 90° analyzing magnet in order to select the desired charge state and energy. In our case we select F^{4+} because it is the most intense ion beam at 5 MV, giving an energy of 25 MeV. The 90° analyzing magnet focusses the beam onto a set of image slits. A portion of the beam striking the image slits produces a current imbalance on the slits due to energy fluctuations in the beam. This current difference between the two image slits can then be sent to a differential amplifier which in turn is fed back to the terminal corona system to stabilize the terminal high voltage. Finally, the switching magnet is used to select among the beam lines set up for different experiments in the target room.

Experimental Set-Up

A schematic diagram of the apparatus is shown in Figure 4. As mentioned previously we have four sections to describe. The recoil-ion source consists of a pusher, nozzle, extracting grid (V_G), a ground grid (G) and an einzel lens.

The dimensions of the recoil-ion source are as follows: the distance between the nozzle and pusher is 1.98 cm, the distance between the nozzle and extracting grid is

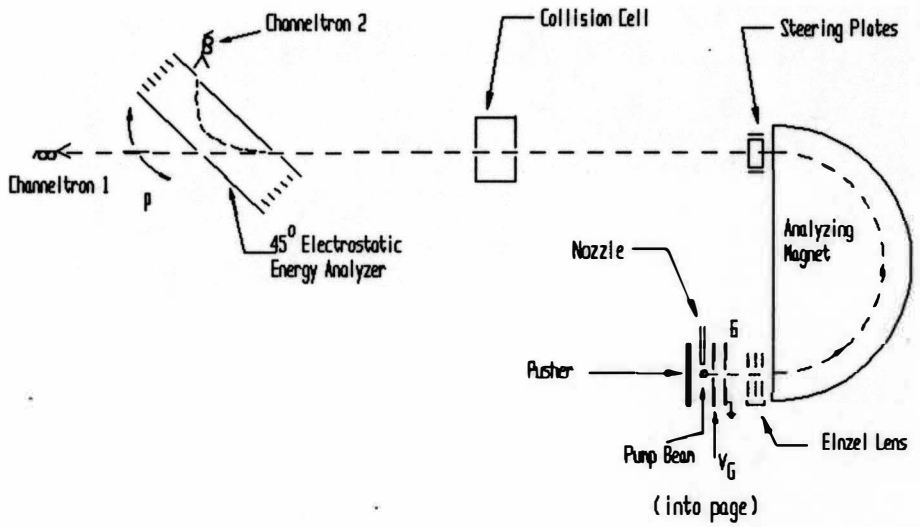

Figure 4. Schematic Diagram of the Experimental Apparatus.

0.82cm and the distance between nozzle and Einzel lens is 4.20 cm.

Multiply-charged ions from rare gas atoms are produced in the recoil-ion source when the fast fluorine beam strikes the rare gas atoms which come from the nozzle. After the fast fluorine beam passes through the interaction region in the recoil-ion source, it is collected by a Faraday cup (FC) (not shown). The residual gas pressure in the main chamber, is around 2×10^{-6} torr. The recoil ions are extracted perpendicular to the fast fluorine beam with an accelerating voltage V_{acc} which is approximately equal to the extracting grid voltage V_G. Typical operating parameters for Ar^{4+} ions and Ne^{3+} ions are given in Table 1. The einzel lens is then used to focus the recoil ions into the

Table 1

Recoil Ion Source Operating Parameters

	Ar^{4+} (Volts)	Ne^{3+} (Volts)
Pusher (P)	197	201
Nozzle (N)	147	155.5
Extracting Grid (V_G)	144	153
Einzel Lens(EL)	134	71.5
Accelerating Voltage	144.75	153.5

analyzing magnet.

Ions extracted from the ion source are mass analyzed by a 180° analyzing magnet of diameter 26 cm. The magnetic field was calibrated using a Hall probe. A typical magnetic current vs. field strength curve is shown in Figure 5. The magnetic field has been found to be fairly uniform except at large magnetic current. After mass analysis, the recoil-ion beam is collimated by a 3mm diameter aperture (not shown in Figure 4) then deflected by the steering plates, to cause them to pass through the collision cell.

In the collision cell, an incident ion may ionize a

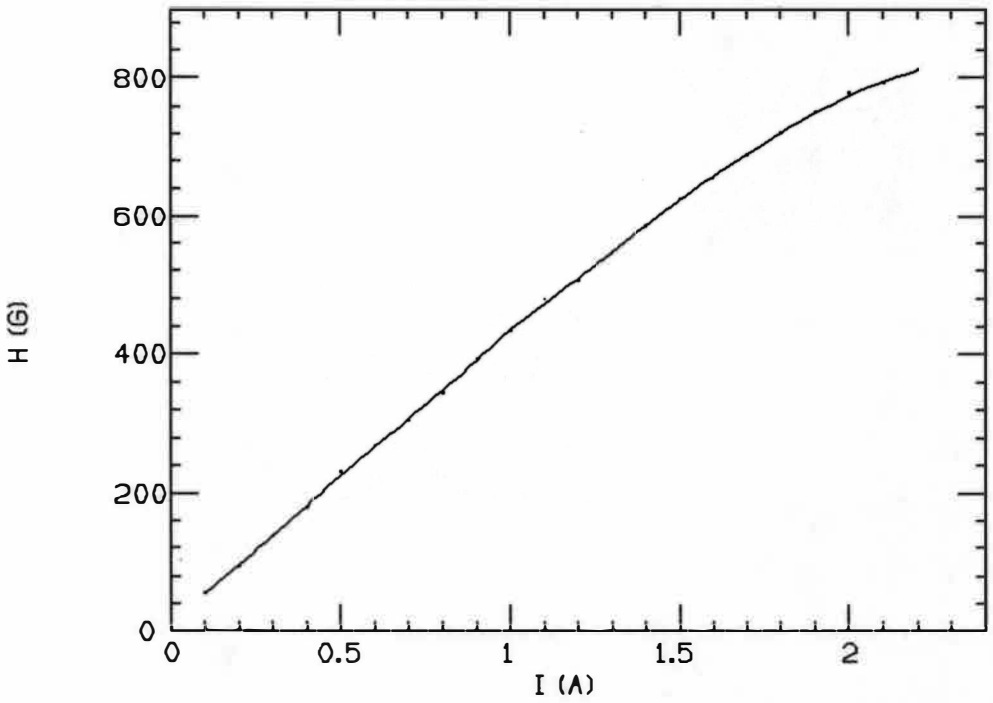

Figure 5. Magnetic Field Current vs. Field Strength Curve.

target gas atom by capturing an electron during a collision. The scattered ion is then energy analyzed by a 45° parallel-plate analyzer and detected by channeltron 2.

Design and Analysis of the Parallel-Plate Analyzer

A uniform electric field is applied between the two parallel plates as shown in Figure 6, where the upper plate is positive. The lower plate is kept at earth potential. Positive ions enter the field at 45° through the first slit and, travelling in parabolic paths, are refocussed upon the exit slit. The behavior of these particles for these conditions has been described by Spangenberg (1948).

The distance between the two plates is 38 mm and the two adjustable slits S1 and S2 are kept at 127 mm apart.

Energy Resolution

The energy resolution of the parallel-plate analyzer is the range of energy, ΔE_o, which ions at average energy E_o may possess and still pass through the two slits of the analyzer with a given value of deflecting voltage. This range of energy ΔE_o will depend on (a) the slit widths ΔX_1 and ΔX_2 of S1 and S2 respectively, (b) the separation between the slits X_o, (c) the range $\Delta\theta$ of entrance angles possible. Figure 7 shows a beam of ions entering the analyzer. Since ions enter at different points within the first slit and at different angles, there is a finite range of energies which they may possess and still pass through the second slit. Shown in Figure 7 are three paths by which an ion may enter; ray 1 enters the center of slit 1 at 45^o with energy E_o, and leaves through the center of slit 2 at 45^o. The ion that can have the highest energy and still pass through slit 2 must enter along ray 2, and the ion that can have the lowest energy and still pass through slit 2 must enter along ray 3. Consequently, ΔE_o will be determined by the difference in energies for rays 3 and 2, which is

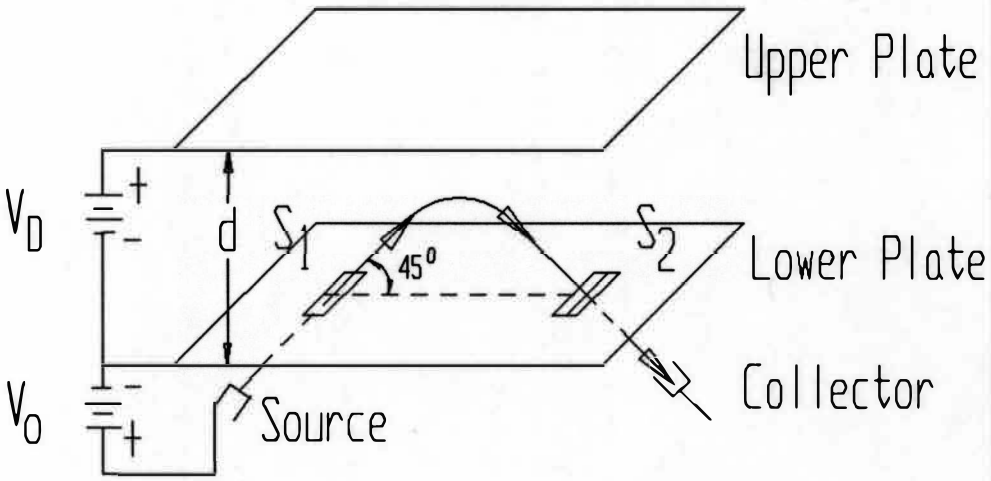

Figure 6. Diagram of the Parallel-Plate Analyzer.

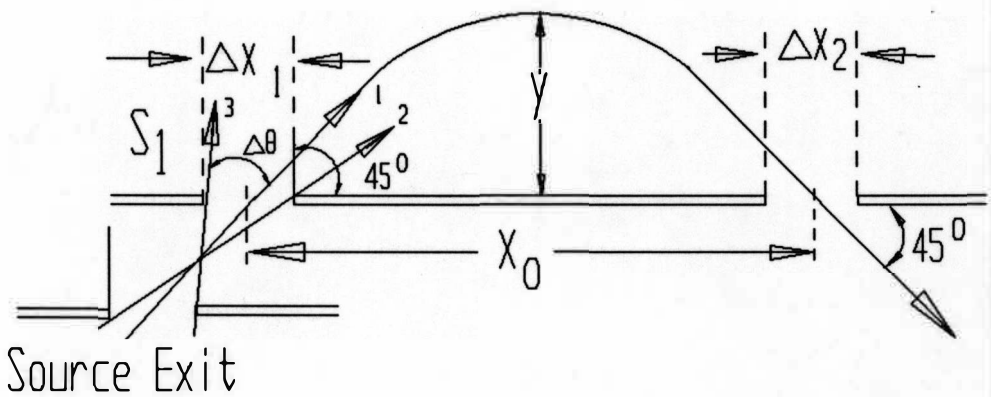

Figure 7. Diagram Used to Determine the Resolution of the Analyzer.

$$\Delta V_0 = V_{0_{max}}(3) - V_{0_{min}}(2) \qquad (3.2)$$

Harrower (1955) has shown that

$$\frac{\Delta V_0}{V_0} = \left[\frac{\Delta X_1 + \Delta X_2}{2X_0}\right]\left[(1+\sec 2\Delta\theta) - (1-\sec 2\Delta\theta)\right] \qquad (3.3)$$

where $\Delta\theta$ is shown in Figure 7.

For the present set up the ion source is far away from the entrance of the parallel-plate analyzer. Then

$$\Delta X_1 = \Delta X_2 = \Delta X \qquad (3.4)$$

$$\Delta\theta = 0^o \qquad (3.5)$$

Therefore

$$\frac{\Delta V_o}{V_o} = \frac{2\Delta X}{X_o} \qquad (3.6)$$

For ΔX = 1 mm and X_0 = 127 mm

$$\frac{\Delta V_0}{V_0} = 1.5\% \qquad (3.7)$$

The deflecting voltage V_D to be used between the parallel plates to deflect a beam of energy $E_0 = qV_{acc}$ (in eV)

entering S_1 at an angle of $\theta=45^{\circ}$ is given by (G.A.Harrower, 1955)

$$V_D=2\frac{d}{X_0}V_{acc} \qquad (3.8)$$

where $V_{acc} = V_0$

d = the separation between the plates

It is generally convenient to restrict θ to 45°. According to Harrower, if $\theta = 42^{\circ}$, the maximum height attained by the ion between the parallel-plate analyzer is $0.224\ X_o$ and if $\theta = 48^{\circ}$ it is $0.275\ X_o$. Therefore with $\theta = 45^{\circ} \pm 3^{\circ}$ the separation of the parallel plates will be adequate if the choice is made

$$d = 0.3\ X_o \qquad (3.9)$$

Then, for the present set up of the analyzer, equation (3.8) reduces to

$$V_D = 0.6\ V_{acc}. \qquad (3.10)$$

It should be emphasized that this relation is linear, so that an energy spectrum in electron volts will be linear against deflecting voltage. This is shown in Figure 8. The slope of this curve is equal to the analyzer constant. In our case

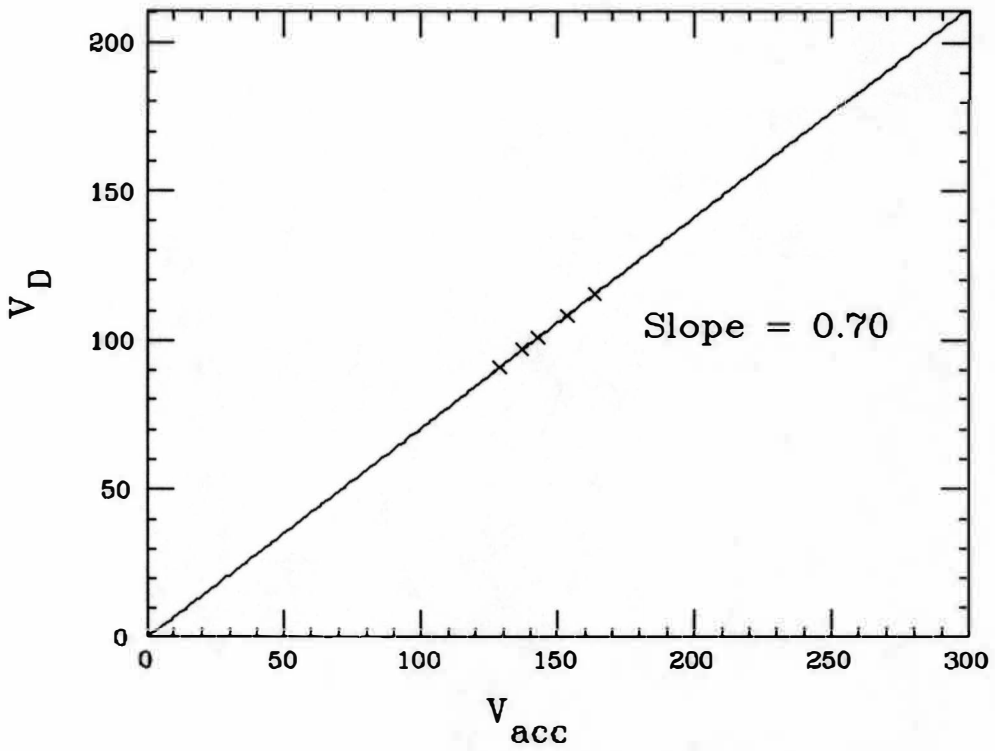

Figure 8. Schematic Diagram Representing the Linear Relationship Between V_D and V_{acc}.

$$V_D = 0.70\ V_{acc}$$

where $k = 0.70$

The differences between the theoretical and the experimental values for k are due to the measurement of the distances d, x_0, and V_{acc}.

Electronics

The electronics block diagram for the energy-gain spectrometer is shown in Figure 9. KSCAN, a program written in FORTRAN for the VAX workstation, controls the

magnetic current and the voltage applied to the parallel-plate analyzer. Commands and data are transferred between the VAX workstation and crate controller over a serial interface. The crate controller is a PDP 11/83 microprocessor based STARBUST unit (Creative Electronic Systems S.A.). It has been programmed to accept and execute the standard set of CAMAC commands. The magnetic current and parallel-plate voltage (V_D) are set by commands to a DAC (digital-to- analog convertor). The DACs have 12 bits, so their resolution is 0.02%. The digitized integrated beam current and channeltron counts are read from the scalers. Using KSCAN the operator can choose to scan stepwise either the magnet or the parallel-plate analyzer. Energy-gain spectra were recorded by scanning the deflecting voltage V_D applied to the parallel-plate analyzer controlled by one of the DACs. The integrated main beam current from the Faraday cup was used to normalize each scan step.

Experimental Procedure

The system is optically aligned using a telescope in a fixed mount. The vacuum system is evacuated by the diffusion pumps until a background pressure of 1.4×10^{-6} torr is obtained. Research grade noble gas of purity 99.995% is introduced into the recoil-ion source through a needle valve which results in an increase in the background

pressure to 3 x 10^{-6} torr. Multiply-charged ions produced in the recoil-ion source are extracted, accelerated, focussed and mass analyzed before passing through the collision cell. By adjusting the deflection and focussing voltages, the beam is made to pass through the analyzer and is monitored by channeltron 1 (see Figure. 4) with no potential difference across the plates of the energy analyzer. For energy analysis, the ion beam is detected by channeltron 2 with the correct voltage across the analyzer. Channeltrons are used as ion detectors because of their stability and long life.

The energy resolution of the parallel-plate electrostatic energy analyzer was measured by changing the voltage across it and measuring the corresponding counts for a fixed time at channeltron 2. A typical energy resolution spectrum is shown in Figure 10. To measure the angular resolution the analyzer voltage is kept fixed for maximum count rate at channeltron 2 and the angular position of the analyzer is changed in steps of 0.125^0. A typical angular resolution of the apparatus is shown in Figure 11, which has 0.3^0 full-width-at-half maximum (FWHM).

A charge-state spectrum of argon recoil ions produced in the recoil-ion source was obtained by varying the current of the 180^0 double-focussing magnet. Figure 12 shows Ar^{q+} recoil ions with charge states ranging from 3+

to 9+ obtained with intensities sufficient for the energy-gain measurement.

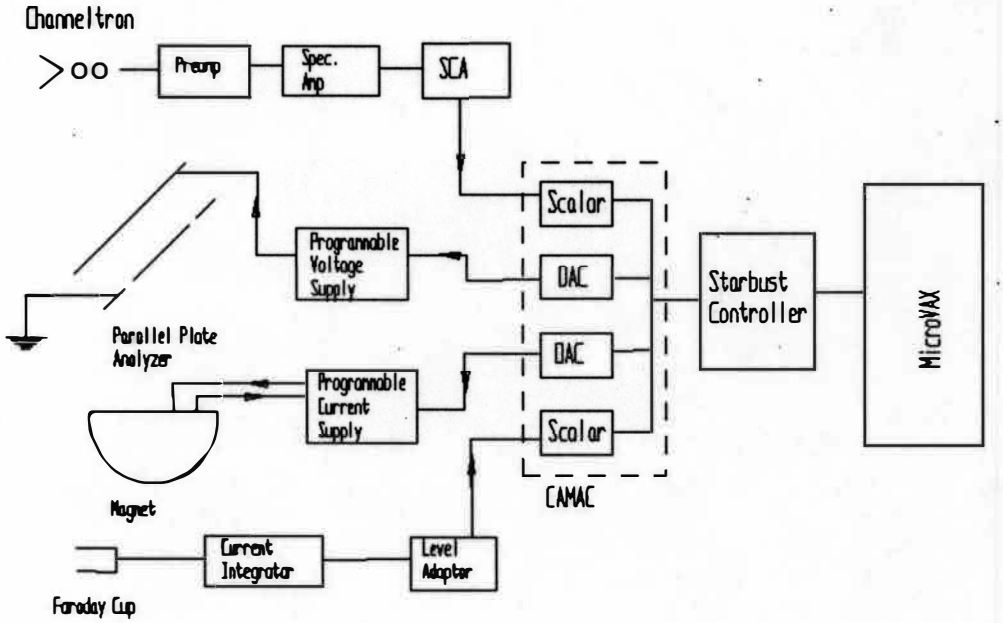

Figure9. Electronic Block Diagram for the Energy-Gain Spectrometer.

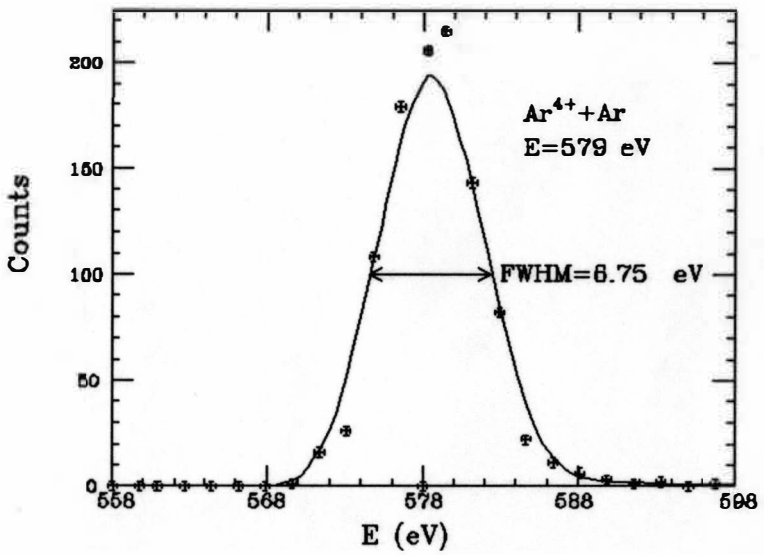

Figure 10. Energy Resolution of the Analyzer. The Full-Width Half-Maximum(FWHM) is 6.75 eV for 579 eV Ar^{4+} Recoil Ions.

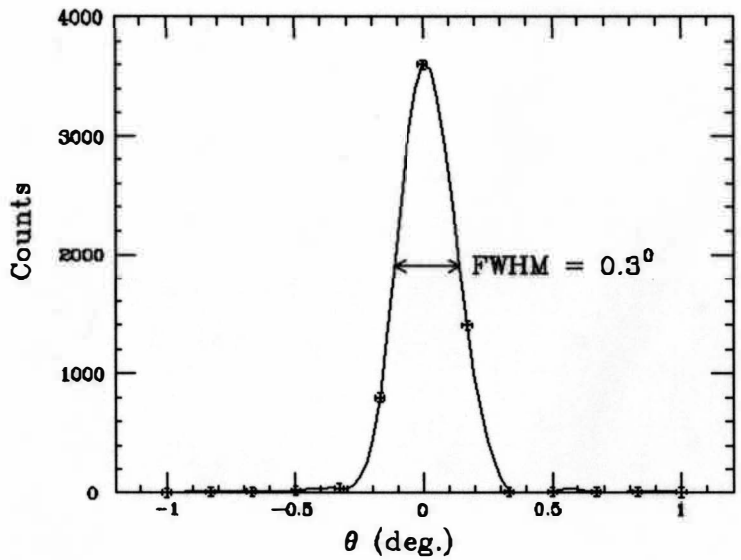

Figure 11. Angular Resolution of the Apparatus.

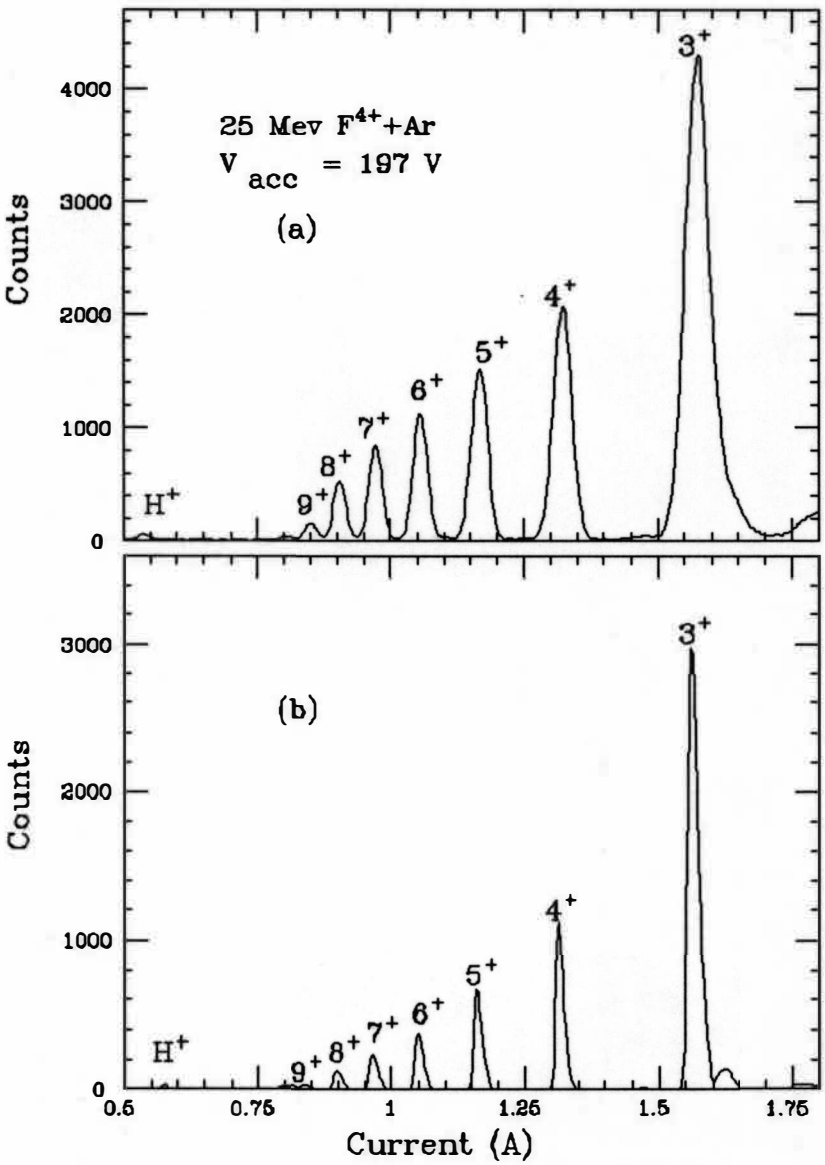

Figure 12. Ar^{q+} Recoil-Ion Charge-State Intensities for 25 Mev F^{4+} Incident on Ar gas as a Function of the Magnetic Current.

(a) Detected by Channeltron 1
(b) Detected by Channeltron 2.

CHAPTER IV

DATA ANALYSIS

The energy gain of the ion can be calculated as follows. We know

$$V_D = k\ V_{acc} \tag{4.1}$$

where k=0.70 is the analyzer constant. Then,

$$V_{acc} = \frac{V_D}{k} = \frac{E}{q} \tag{4.2}$$

where q is the charge of the projectile. For charge q′ where q′ = q - 1, the energy gain of the projectile following single-electron capture is

$$Q = E' - E$$

$$Q = q'\left[\frac{V_D'}{k}\right] - q\left[\frac{V_D}{k}\right] \tag{4.5}$$

$$Q = q'\left[\frac{V_D'}{V_D}\right] V_{acc} - qV_{acc} \tag{4.6}$$

$$Q = V_{acc}\left[\frac{q'V_D'}{V_D} - q\right] \tag{4.7}$$

$$Q = V_{acc} q \left[\frac{q' V_D'}{q V_D} - 1 \right] \qquad (4.8)$$

The above equation for the energy gain Q corresponding to V_{acc} is from Kamber et al. (1987a).

For Q = 0;

$$\frac{q' V_D'}{q V_D} = 1 \qquad (4.8)$$

or

$$V_D = \frac{V_D}{q'} q \qquad (4.9)$$

From the above equation one can find V_D', the voltage applied to the parallel-plate analyzer for charge q′ if one knows V_D, q and q′. The energy defects for possible exit channels were determined from published compilations of energy levels (Bashkin and Stoner 1978) using equation (2.2). In the present work, the translational energy spectra are expressed in terms of the Q values.

CHAPTER V

RESULTS AND DISCUSSION

In this chapter, the results of selected collision systems are presented and discussed.

Ar^{4+} - Ar Collision system

Figure 13 shows translational energy-gain spectra obtained for single-electron capture by 579 eV Ar^{4+} ions from Ar at different scattering angles. One can see a broad peak centered around 8 eV. From equation (2.10) this corresponds to a curve crossing at R_x = 10.2 a.u. where R_x = (q-1)27.2/Q(eV) (neglecting polarization), (Dalgarno, A. and Butler, S.E. 1978). This process correlates with single-electron capture into the 4p state of Ar^{3+} from ground state incident Ar^{4+} ($3P^2$ ^3P) (Bashkin and Stoner 1978). There might also be some unresolved contributions from capture into 4s and 3d states.

Previous measurements by Giese et al. (1986) for the same collision system at 2180 eV, shows that the dominant peak is also due to the capture into the 4p state. Puerta et al. (1985) also studied this collision system at 800 eV impact energy. Their result shows that the reaction channel due to capture into the 4p state is predominant;

and the recent results of Biedermann et al. (1990) also show good agreement with our measurements.

Figure 13 also shows the reaction windows calculated on the basis of a single-crossing Landau-Zener model using the values of H_{12} containing Taulbjerg factors $f_{nl} = 1$ (broken lines) and $f_{nl}(4p) = 0.671$ (dotted lines). In this study the maximum cross sections obtained from theoretical calculations are normalized to the observed dominant peak values in the energy gain spectra. The reaction windows based on $f_{nl} = 1$ and $f_{nl}(4p) = 0.671$, calculated for capture into the 4p state, provide the best description of the dominant process.

As the projectile scattering angle is increased, capture into the 4p state of Ar^{3+} remains dominant, but contributions from large Q-values make their appearance as would be expected.

Figure 14 displays the measured total differential cross sections for single-electron capture by Ar^{4+} ions from Ar at a collision energy of 579 eV. The differential cross sections ($d\sigma/d\Omega$) were found by calculating the area under the peaks (Figure 13) using a curve fitting program. The data show that the distribution for single-electron capture is peaked at an angle of $0.18^0 \pm 0.15^0$ and for larger angles is a monotonically decreasing function. The data also show that the projectile products are distributed mostly at

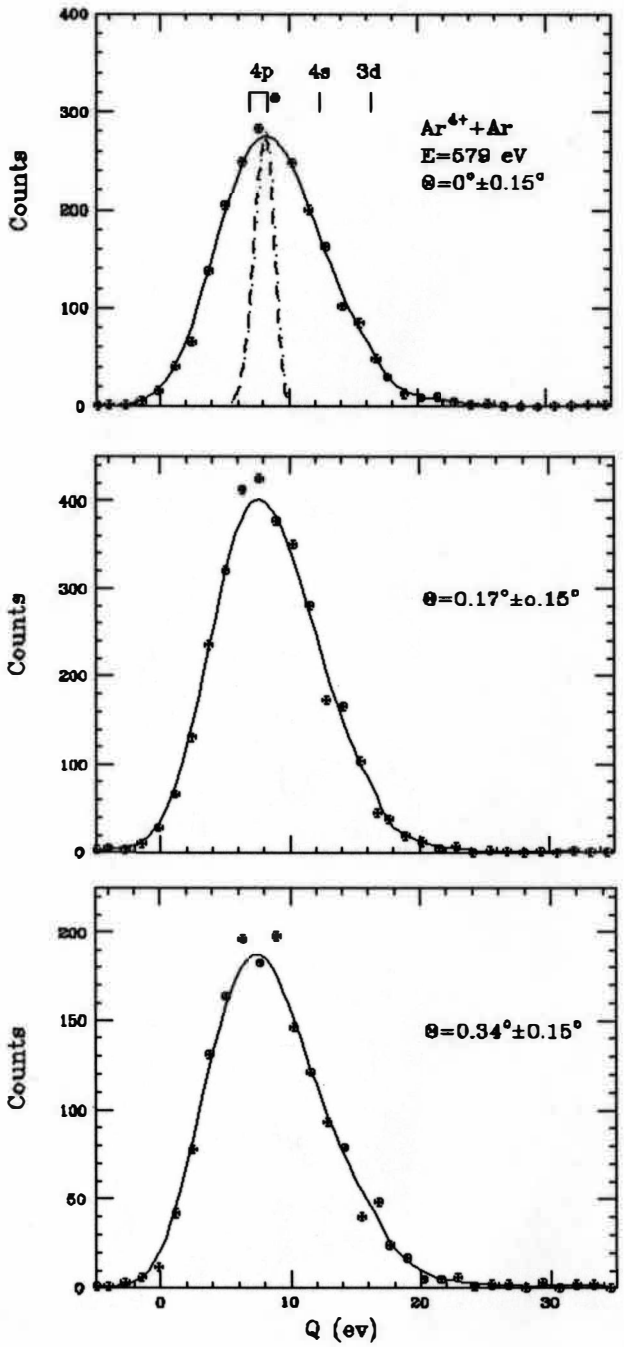

Figure 13. Translational Energy-Gain Spectra for Single-Electron Capture by 579 eV Ar^{4+} Ions from Ar at Different Scattering Angles. --- f_{nl} = 1, ... f_{nl} = 0.637.

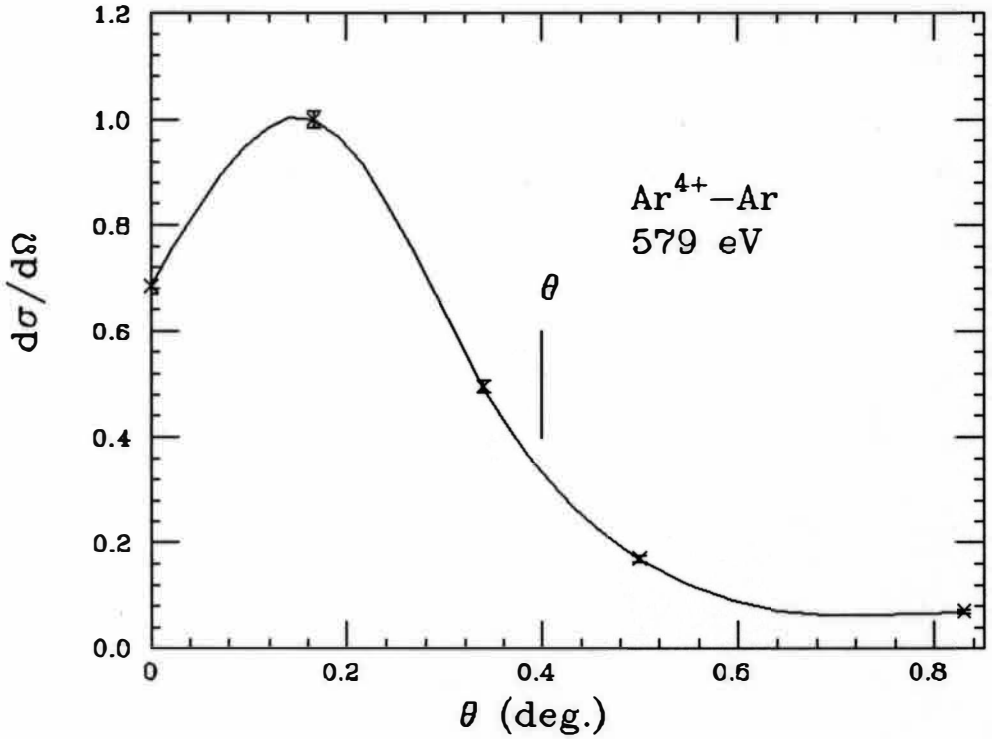

Figure 14. Total Differential Cross Sections for Single-Electron Capture by 579 eV Ar^{4+} ions from Ar.

angles smaller than $\theta = 0.4^0$, which corresponds to the 4p capture channel at an impact parameter equal to the crossing radius, from equation (2.5).

Ne^{3+} - He Collision System

Figure 15 shows the translational energy-gain spectra for single-electron capture by 460 eV Ne^{3+} ions from He at 0^0 and 1^0. At 0^0 scattering angle, the spectrum exhibits one broad peak. This peak is due to single-electron capture into the $2p^3\ ^2P$ metastable state of Ne^{3+} forming the $3s'\ ^{5,3}S$ state of Ne^{2+} (Bashkin and Stoner 1978). This

process is exothermic by 5 eV with a curve crossing at R_x = 10.9 a.u (from equation 2.11). There are also some contributions from capture into the $2p^3\ ^4S$ ground state of Ne^{3+} forming the $2p^5\ ^1P$ state of Ne^{2+}. Reaction windows based on f_{nl} = 1 (broken line) and f_{nl} (3s') = 0.866 (dotted line) are also shown in Figure 15. Here, it can be seen that neither reaction window describes the position of the dominant process. At a scattering angle of 1^0, a second peak due to capture into the ground state Ne^{3+} forming the $2s2p^5\ ^3P$ state of Ne^{2+} is observed (Bashkin and Stoner 1978). This can only be explained due to core-varying (i.e., an inner shell is altered) single-electron capture transitions, since the final Ne^{2+} ($2s2p^5$) state cannot be described by a single configuration state (Winter 1991). Such a core-varying process can be produced when excitation of the projectile ion and capture of a target electron occur simultaneously. Such a process, is called 'transfer excitation (TE)' (Winter 1991).

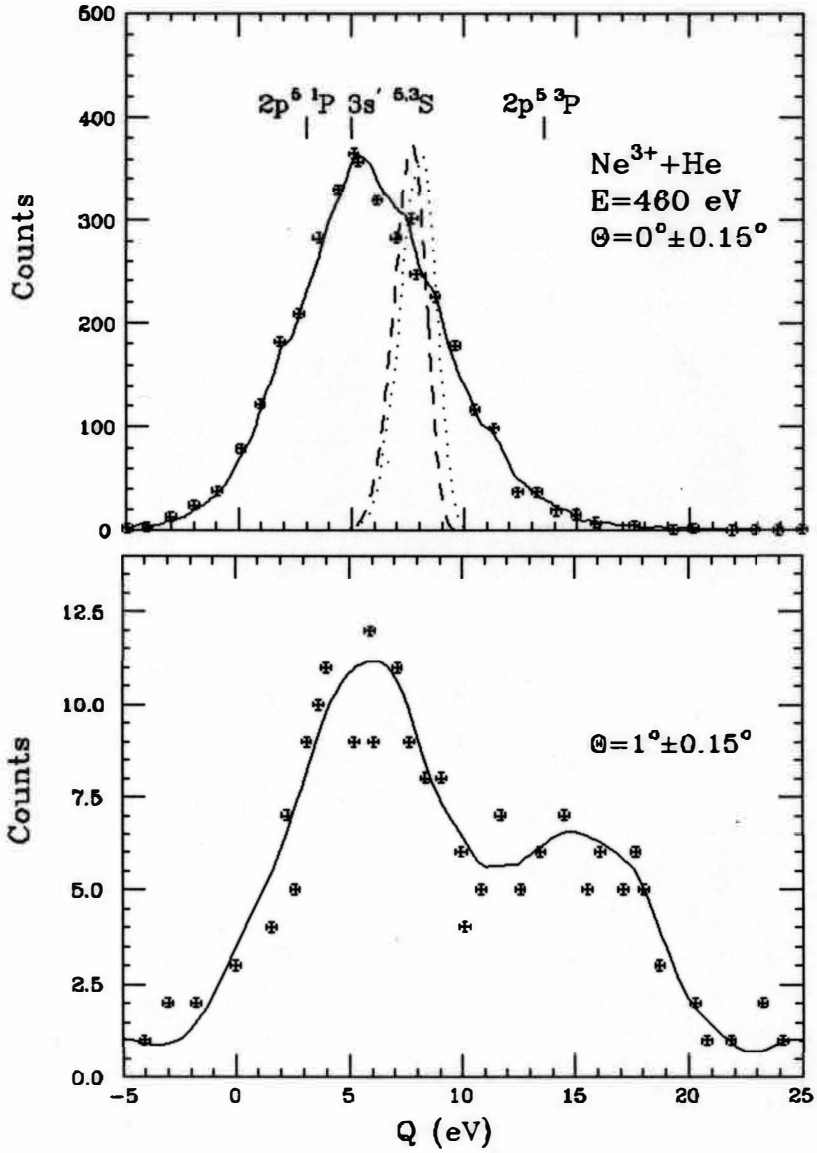

Figure 15. Translational Energy-Gain Spectra for Single-Electron Capture by 460 eV Ne^{3+} Ions from He at Scattering Angles of 0^o and 1^o. ---- f_{nl} = 1, ... f_{nl} = 0.866.

CHAPTER VI

CONCLUSION

The main objective of this thesis was to describe a new apparatus which will enable the study of double differential cross sections for electron capture processes by low-energy multiply charged ions. For the collision systems studied (Ar^{4+} - Ar and Ne^{3+} - He) capture is found to selectively populate states for curve crossings occurring at 10.2 and 10.9 a.u. respectively. The experimental results show good agreement with predictions of the single-crossing Landau-Zener model (Kamber et al., 1991) for Ar^{4+} + Ar collisions, while for Ne^{3+} + He collisions the model predicts the position of the dominant reaction channel to be at 6.9 a.u., smaller than the experimental result. As the projectile scattering angle is increased, the peak for the dominant reaction channel broadens and contributions from large Q-values make their appearance, as would be expected in smaller impact parameter collisions.

Finally, in considering methods that might be employed to improve and extend the present measurements, one could proceed in several directions. Most important is to improve the energy resolution of the analyzer by reducing the widths of the entrance and exit slits to resolve the

separate exit channels in a collision process, such as the systems studied here in this work. Next, this can also be accomplished by retarding the scattered ions to lower energies before they enter the energy analyzer. Another improvement would be to modify the present apparatus for coincident translational energy-gain spectroscopy in which the scattering angle and the energy-gain spectrum of the capturing projectile can be measured simultaneously in coincidence with the recoil ion. The latter method will provide detailed information and a better understanding of the influence of angular scattering effects on the structure of energy spectra.

BIBLIOGRAPHY

Afrosimov, V. V., Basalaev, A. A., Panov, M. N., & Samoilov, A. V. (1986). Electron Capture from helium atoms into various electronic states by multiply charged argon ions. Soviet Physics JETP, 64, 273.

Baskin, S., & Stoner, J. O. (1978) Atomic energy levels and Grotrian Diagrams. Amsterdam:North-Holland.

Biedermann, C., Cederquist, H., Anderson, L., Levin, J. C., Short, R. T., Elston, S. B., Gibbons, J, D., Anderson, H., Liljeby, L., Sellin, I. A., (1990). Experimental and Model Angular Distribution of one- and two-electron Capture Processes in 0.5-20 eV Ar^{4+} - Ar collisions. Physical Review A, 41, 5889.

Carolan, P. G., Duval, B. P., Field, A. R., Fielding, S. J., Hawkes, N. C., Peacock, N. J., Fussmann, G., Janeschitz, G., Hofmann, J., Behringer, K. H., Isler, R. C., (1987). Charge-exchange-excited line radiation in a tokamak with neutral-particle-beam injection. Physical Review, A35, 3454-3471.

Cocke, C. L., Kamber, E. Y., Tunnel, L. N., Varghese, S. L., & Waggoner, W. (1987). Angular distribution of reaction products from low energy capture by multicharged ions. Nuclear Instruments and Methods in Physics Research, A262, 89.

Cooks, R. G. (1978). Collision Spectroscopy. New York: Plenum Press.

Creative Electronic Systems S.A. Route du Point Butin 70, Petit Lancy CH1213, Geneva, Switzerland.

Dalgarno, A. (1985). Charge transfer process in astrophysical plasmas. Nuclear Instruments and methods in physics Research, B9, 655.

Dalgarno, A., & Butler, S. E. (1978). Charge transfer of multiply-ionized species. Comments on Atomic and Molecular Physics, 7, 129

Donne, A. J. H., De Heer, F. J., (1987). The role of charge-changing collisions with impurity ions in active-

beam plasma diagnostics. Nuclear instruments & Methods in Physics Research, B23, 219-221.

Drawin, H. W., (1981). Atomic Physics and Thermonuclear Fusion Research. Physica Scripta, 24, 622-655.

Duval, B. P., Hawkes, N.C., Fielding, S. J., Isler, R. C., and Peacock, N. J., (1985). Charge exchange observations and analysis in the dite Tokamak. Nuclear Instruments and Methods in Physics Research, B9, 689-697.

Giese, J. P., Cocke, C. L., Waggoner, W. T., Tunnel, L. N., & Varghese, S. L. (1986). Energy-gain spectroscopy of electron-capture collisions between low-energy Ar and Ne projectiles and atomic and molecular deuterium targets. Physical Review A, 34, 3770.

Harrower, G. A. (1955). Measurement of electron energies by deflection in a uniform electric field. Review of Scientific Instruments, 26, 850.

Isler, R. C., Morgan, P. D., Peacock, N. J., (1985). Impurity Accumulation in ISX-B during counter-injection-Are alternative hypothesis valid?. Nuclear Fusion, 25, 386-392.

Kamber, E. Y., Cocke, C. L., (1991). Ion-Neutral Reactions:Collision Spectrometry of multiply charged ions at low energies. Springer series in chemical physics 54, 91-122.

Kamber, E. Y., Cocke, C. L., Giese, J. P., Pedersen, J. O. K., and Waggoner, W., (1987a). An experimental appara tus for studying double differential scattering by low energy X^{q+} ions from He. Nuclear Instruments and Methods in Physics Research, 24/25, 288-290.

Kamber, E. Y., Cocke, C. L., Giese, J. P., Pederson, J. O. K., & Waggoner, W. (1987b). State-selective differen tial single-electron capture cross sections for O^{2+} - He collisions. Physical Review A, 36, 5575.

Kimura, M., Iwaim, T., Kobayashi, N., Matsumoto, A., Ohtani, S., Okuno, K., Takagi, S., Tawara, H., & Tsurubuchi, S. (1984). Landau-Zener Model calculations of one electron capture from He atoms by highly stripped ions at low energies. Journal of the Physical Society of Japan 53, 7, 2224.

Landau, L. D. (1932). Energy calculations of diabatic

crossings. Physics Z. Soviet Union, 2, 46.

McCullough, R. W., Wilson, S. M., & Gilbody, H. B. (1987). State-selective capture by slow Ar^{4+}, Ar^{5+} and Ar^{6+} recoil ions in H, H_2 and He. Journal of Physics B, 20, 2031.

Nielsen, E. H., Anderson, L. H., Barany, A., Cederquist, H., Heinnemeir, J., Hvelplund, P., Kundsen, H., MacAdam, K. B., & Sorensen, J. (1985). Energy-gain spectroscopy of state-selective electron capture for multiply charged Ar recoil ions. Journal of Physics B, 18, 1979.

Olson, R.E., & Kimura, M. (1982). Angular Scattering in slow multiply-charged ion, atom collisions. Journal of Physics B, 15, 4231.

Olson, R. E., & Salop, A., (1975). Charge exchange between H(1S) & fully stripped heavy ions at low-keV impact energies. Physical Review A, 13, 1312.

Olson, R. E., & Salop, A. (1976). Electron transfer between multicharged ions and neutral species. physical review A, 14, 579.

Peacock, N. J., Summers, H. P., (1987). Level inversion in multiply charged ions and possible applications. Nuclear Instruments & Methods in Physics Research, B23, 226-233.

Puerta, J., Kahlert, H. J., Koslowski, H. R. & Huber, B. A. (1985).Single electron capture by state-selected multiply charged $^{q+}$ ions (q = 3,4). Nuclear Instrumental Methods B, 9, 415.

Spangenberg, K. R., (1948). Vacuum Tubes, McGraw-Hill: New York p100.

Suckewar, S., (1981) Spectroscopic Diagnostics of Tokamak Plasmas, Physica Scripta 23, 72-86.

Taulbjerg, K. (1986). Reaction windows for electron capture by highly charged ions. Journal of Physics B, 19, 1367.

Winter, H. (1991). Two-electron transitions in single electron capture from atoms by slow doubly charged ions. Comments on Atomic Molecular Physics, 27, 3299.

Yaltkaya, S., Kamber, E, Y., and Ferguson, S, M., (1993).

Double differential cross-sections for state-selective electron cpature low-energy Ar^{q+} ions from He and Ar. Physical Review A, 48, 382.